Mavromatis *et al.*
*European Transport Research Review* (2023) 15:8
https://doi.org/10.1186/s12544-023-00582-5

European Transport Research Review

ORIGINAL PAPER

Open Access

# An evaluation of the passing process through road - vehicle parameters assessment

Stergios Mavromatis[1], Vassilios Matragos[1*], Konstantinos Apostoleris[2], Fotios Fotos[1] and George Yannis[1]

## Abstract

**Purpose** This paper investigates the interaction between vehicle dynamics parameters and road geometry during the passing process.

**Methodology** The methodology is based on a realistic representation of the passing task with respect to roadway's posted speed and the ability of the passing (examined) vehicle to perform such maneuvers. Regarding passing distance outputs, an existing vehicle dynamics model was utilized, where aiming to assess the model's accuracy, instrumented field measurements were performed. The analytical model is computationally demanding. Therefore statistical models were worked out, in line with the German rural road design guidelines, to determine passing sight distances (PSDs) by arranging combinations of 4 critical vehicle—roadway parameters; namely, vehicle horsepower rates, variations between the passed vehicle's speed and roadway's posted speed, peak friction supply coefficients and grade values.

**Results** The analysis revealed that the difference between the speed of the passed vehicle and the posted speed value, as well as certain interactions of the assessed parameters impact excessively PSD, especially for values below 20 km/h. The lognormal modelling approach for predicting PSDs was found efficient and may be useful to researchers and practitioners aiming to evaluate the interaction of the utilized road—vehicle parameters in terms of determining PSDs as well as passing zones.

**Conclusions** Although more advanced communication between vehicles or between vehicles and road environment seems a prerequisite in order integrated guidance during passing maneuvers to be enabled, the present research consists an opening paradigm of how the passing process can be standardized and therefore deployed in advanced driver assistance systems (ADAS).

**Keywords** Passing sight distance, ADAS, Passing maneuver, PSD assessment, Road design guidelines

## 1 Introduction

Two lane rural roads have the highest proportion of accidents [9]. In terms of accident severity, accidents associated with failure during the passing process, such as head-on collisions or collisions between the passing and the passed vehicle driving in the same direction, seem to prevail (e.g. [4, 25, 27, 29]).

Passing is permissible on specific road areas (passing zones). The locations with passing zones strongly depend on the provision of at least minimum sight distance [passing sight distance (PSD)]. PSD is the distance that drivers must be able to see along the road ahead to safely and efficiently initiate and complete passing maneuvers of slower vehicles on two-lane rural roads using the lane normally reserved for opposing traffic [31].

Road geometric design has a vital role in the provision of adequate PSDs. Passing is usually performed on tangents and rather wide curves in terms of curvature.

*Correspondence:
Vassilios Matragos
vasmatragos@mail.ntua.gr
[1] School of Civil Engineering, National Technical University of Athens, 15773 Athens, Greece
[2] School of Rural, Surveying and Geoinformatics Engineering, National Technical University of Athens, 15773 Athens, Greece

However, in such areas the presence of grades and more particularly crest vertical curves may impose additional barriers. The respective assessment revealed that the boundaries of PSD inadequacy are concentrated in advance and inside the vertical curve. More detailed quantification can be found in Mavromatis and Markos [20].

Road sections with limited passing opportunities besides safety impose also operational degradation. Such cases might motivate certain drivers to make risky passing attempts either late in a passing zone or on a portion of the road not intended for passing and therefore seem mostly critical [2].

The most effective mean to eliminate such accidents is to provide additional passing lanes, or at least protected passing zones through the provision of continuous 3-lane cross-section (2 + 1 roads). However, such arrangements are not possible for every road environment due to economic, topographical or environmental protection constraints [33]. Therefore, PSD is a vital design element, which directly imposes economic as well as safety and operational considerations.

The technological advancements provided by connected vehicles (CVs) and autonomous vehicles (AVs) are paving the way for a more "tailored" interaction between vehicle(s) and road environment. At present, vehicles equipped with Level 2 automation (partial automation) as defined by the society of automotive engineers (SAE) [30] are already in the market, although mainly their contribution is limited to controlled conditions such as rather smooth geometric design [11].

In view of the deployment of such advanced driver assistance systems (ADAS) in the near future, the objective of the paper is to investigate the interaction between vehicle dynamic parameters and road geometry during the passing process. The authors intend to deliver passing distance outcomes as a function of critical vehicle and road parameters by analyzing the ability of the examined vehicle to perform passing maneuvers, where as a more generic outcome, statistical models for predicting PSDs are developed.

## 2 Overview of literature

A wide number of research related to the passing process can be found in the literature and many models relating the involved parameters have been calibrated. In many of them passing maneuver data were collected either through an instrumented vehicle, which represented the passing vehicle (e.g. [3, 18]), or from video recording (e.g. [13, 17, 28]), where the overall aim was to assess the relevant distance, time and speed parameters. Some authors utilized driving simulators as well in order to support their findings (e.g. [2, 16]). The advantage of driving simulators experiments, besides providing demographic information of the drivers (e.g. [8, 34]), is that such assessments deliver very accurate data related to the passing task [16].

In terms of modelling passing zones and PSDs, although most of the relevant research studies have reported numerous interesting results, due to the disparity of the directly involved parameters, the proposed passing distance values are extracted based on rather critical assumptions and therefore should be treated with caution. For example, in many studies the speed of the passing vehicle, or the speed differential between the passing and the passed vehicle is considered constant, where in others, acceleration data, although not at all easy to measure, are considered stable as well or in some cases assessed through the measured passing time. The same applies in current road design practice, where many assumptions are being adopted as well.

In AASTHO design guidelines [1], PSD is based on field observations and expressed as the outcome of four different distance components; namely,

- $d_1$, distance traveled during perception and reaction time and initial acceleration
- $d_2$, distance traveled while the passing vehicle occupies the left lane
- $d_3$, distance between passing and opposing vehicle at the end of the maneuver (safety margin)
- $d_4$, distance traveled by an opposing vehicle (2/3 of $d_2$)

The adopted PSD values (Table 1) are based on certain combinations of "assumed" speeds between the passing and the passed vehicle utilizing a speed differential of 19 km/h (12 mph).

In the German RAL, 2012 design guidelines [6], PSD depends on the homogeneity of the proposed road design classes and no longer on speed, where as a result the required PSD is set to 600 m. This value of 600 m has

**Table 1** PSD values for two lane rural roads [1]

| Design speed (km/h) | Assumed speeds (km/h) | | PSD (m) |
|---|---|---|---|
| | Passed vehicle | Passing vehicle | |
| 50 | 31 | 50 | 160 |
| 60 | 41 | 60 | 180 |
| 70 | 51 | 70 | 210 |
| 80 | 61 | 80 | 245 |
| 90 | 71 | 90 | 280 |
| 100 | 81 | 100 | 320 |

evolved from the PSD requirement of a passenger car at 100 km/h attempting to perform a passing maneuver to a truck driven at 70 km/h, while at the same time, at the opposing traffic stream, another passenger car is running at 100 km/h. The required PSD is the sum of the distances covered by the two passenger cars plus a safety margin distance of 100 m.

Safety during the passing process can be violated by many means. Besides operational constraints imposed from traffic volumes and/or traffic composition, the impact of short passing zones, although not extensively validated by accident data seems to be very important in terms of smooth versus violent return of the passing vehicle to the through lane. A recent study [13] showed that in short passing zones, 92% of passing maneuvers ended beyond the passing zone, compared to 21% of longer passing zones (over 300 m). A similar research [10] revealed that the proportion of forced and violent returns for 270 m long passing zone was 10%, and it increased to 45% at 200 m long passing zone. Another issue of concern is that in many research studies (e.g. [2, 26]), the speeds of passing vehicles were found to be over the posted speed.

From the above it is more than evident that the passing process is a complex task, where the recommendations provided from the existing analyses unavoidably are rather widespread. At the same time, it is widely accepted that the conventional approach for improving safety seems to be constantly moving towards the benefits of automation.

## 3 Methodology

The proposed PSD investigation is based on a safe and realistic representation of the passing process on tangent road sections, where the actual capacity of the passing vehicle to perform a passing maneuver was examined.

The ability of a vehicle to accelerate has already been addressed in previous research of the authors [21–23] where aiming to assess vehicle safety from the interaction between road geometry, tire—pavement friction and vehicle parameters a vehicle dynamics model was developed. More specifically, vehicle acceleration, among other parameters, was associated to the available horsepower rate on the wheels through the horsepower utilization factor "n" (%) since a vehicle cannot always be driven at full horsepower rate.

The following sub-section provides a brief discussion on how the model was structured, where more details regarding the full equations description are available through references [21–23].

It is worth mentioning that in the vehicle's dynamics model and of course within the present analysis, the acceleration is not considered constant.

### 3.1 Vehicle dynamics approach

All forces and moments applied to the vehicle were analyzed into a moving three-dimensional coordinate system, coinciding at the vehicle gravity center and formed by the vehicle's longitudinal (X), lateral (Y) and vertical (Z). Through these axes, the impact of certain vehicle technical characteristics, road geometry and tire friction were expressed, such as: vehicle speed/wheel drive/sprung and unsprung mass and it's position of gravity center/aerodynamic drag/vertical lift/track width/wheel-base/roll center/suspension roll stiffness/cornering stiffness/grade/superelevation rate/rolling resistance tire-road adhesion values and horsepower supply.

Moreover, the model takes into account variables related to vehicle steering and tire sideslip angles [12], the actual wheel load due to the lateral load transfer as well as the corresponding alteration of the lateral force on each wheel, thus creating a four-wheel vehicle dynamics modelling [5, 12, 15]. The model's outputs were validated against the known data derived by two other distinct cases: the final climbing speed of a truck travelling on a grade [19] and the output data from the well-known CARSIM Simulation Software [24]. Both cases revealed a satisfying match.

The available tractive effort of the vehicle (driving force minus rolling resistance) acting on the front or rear axle (depending on the driving configuration) was associated to the vehicle's speed as well as the net power available at the driving wheels. Since a vehicle cannot always be driven at 100% of its available horsepower rate, the horsepower utilization factor (n) was introduced and the following equation applies:

$$Fx = 745.60\frac{P}{V}\frac{n}{100} \tag{1}$$

where: $F_x$: tractive force (Nt), P: net engine horsepower available at the driven axle (around 94% of the nominal value [14]) (hp), v: vehicle speed (m/sec), n: horsepower utilization factor (%)

By applying laws of mechanics, the vehicle's instant acceleration, which is expressed as a four-degree polynomial equation, can be formed as a function of vehicle's instant speed as well as driven distance, thus delivering the following differential equation which is resolved by utilizing numerical Runge–Kutta method [7]:

$$a(v) = \frac{dv}{dd}v \tag{2}$$

where a(v): acceleration ($m/s^2$), v: speed (m/s), d: distance (m).

The solution of Eq. (2) delivers the vehicle speed variation as a function of the required distance. This procedure takes place at impending skid conditions by pairing the determined demanded longitudinal friction ($f_{Tdem}$) to the provided friction supply of the roadway ($f_{max}$) and adapting each time the horsepower utilization factor n from Eq. (1).

It is evident that during vehicle's tractive mode, irrespective of whether the vehicle utilizes or not the total net engine horsepower (n = 100%, or n < 100%), the vehicle increases the speed, which means that acceleration rate decreases.

As long as the vehicle utilizes part of the total net engine horsepower (n < 100%), the vehicle is driven at impending skid conditions, since any increase of "n" will deliver vehicle skidding.

However, when n = 100%, although the vehicle cannot utilize additional horsepower, the speed of the vehicle continues to increase due to acceleration presence, but at a lower rate, since the total amount of available horsepower is continuously utilized. For the same reason, the acceleration drops more rapidly. From that point on, the vehicle is no longer driven at impending skid.

The above can be seen through Fig. 1, where the accelerating performance of a C-class passenger car (KIA Proceed) as a function of the driven distance is shown. Regarding the utilized vehicle parameters (Table 2, second column), although an effort was made to provide them from the vehicle industry (bolded values), most of them were taken from the literature [5]. The engine horsepower was assumed to be 80 hp for the above run.

The initial speed of the vehicle was assumed $V_o = 80$ km/h, the friction supply was set to the unfavorable value of $f_{max} = 0.35$, and the road gradient was assumed 5.50% upgrade. The breakpoint in terms of distance travelled, where the vehicle reaches 100% horsepower utilization (red line) is shown through a dashed vertical line (distance = 68 m). It can be seen that prior to that point the vehicle was accelerating at impending skid conditions (orange line with $f_{Tdem} = 0.35$), where beyond 68 m from the starting point of the assessment, the vehicle speed and acceleration continue growing and reducing respectively with evidently different rates.

### 3.2 PSD assessment

The analysis aims to deliver a tool for standardizing the passing process in view of the continuously evolving

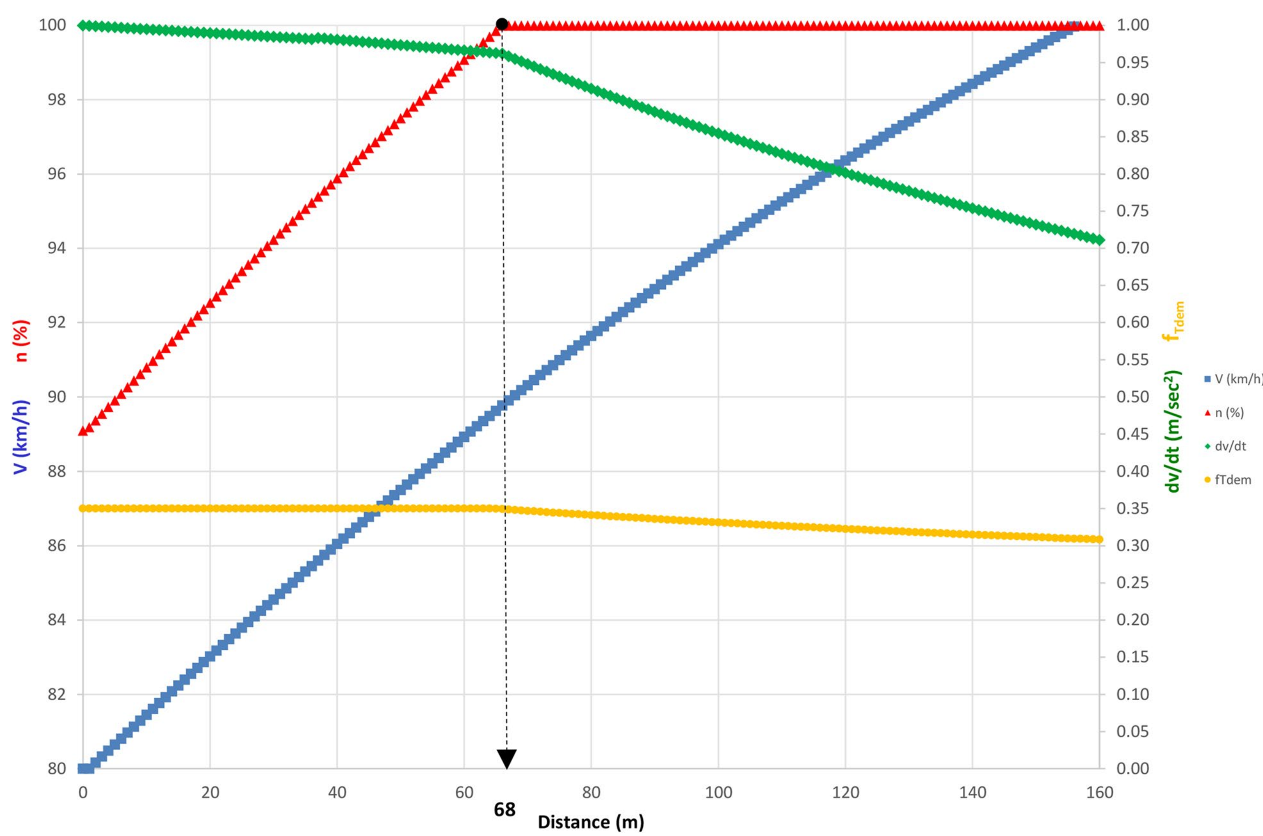


**Fig. 1** Speed–horsepower utilization and acceleration–friction variation versus distance ($V_o = 80$ km/h, P = 80 hp, s = 5.50%, $f_{max} = 0.35$)

**Table 2** Vehicle parameters inserted to the model

| | C class KIA proceed | C class Toyota CH-R | B class Toyota yaris | |
|---|---|---|---|---|
| L (m) | **2.650** | **2.640** | **2.510** | Wheelbase |
| $t_f$ (m) | **1.538** | **1.550** | **1.470** | Front track width |
| $t_r$ (m) | **1.536** | **1.570** | **1.460** | Rear track width |
| m (kgr) | **1300** | **1500** | **1150** | Vehicle mass |
| $l_f$ (m) | 1.161 | 1.161 | 1.031 | Position of GC from front axle |
| h (m) | 0.620 | 0.620 | 0.610 | Position of GC from surface |
| $K_{\varphi f}$ (Nm/rad) | 27,502 | 27,502 | 19,882 | Suspension roll stiffness (front) |
| $K_{\varphi r}$ (Nm/rad) | 14,324 | 14,324 | 9282 | Suspension roll stiffness (rear) |
| $C_{af}$ (kp/rad) | 2295.7 | 2295.7 | 2867.1 | Cornering coef. (front) |
| $C_{ar}$ (kp/rad) | 2120.7 | 2120.7 | 2316.8 | Cornering coef. (rear) |
| $m_{uf}$ (kgr) | 92 | 92 | 80 | Unsprung mass (front) |
| $m_{ur}$ (kgr) | 120 | 120 | 72 | Unsprung mass (rear) |
| $h_{Rf}$ (m) | 0.020 | 0.020 | 0.190 | Roll center height (front) |
| $h_{Rr}$ (m) | 0.410 | 0.410 | 0.190 | Roll center height (rear) |
| $r_{dyn}$ (m) | 0.290 | 0.290 | 0.260 | Dynamic radius |
| $A_f$ ($m^2$) | 1.850 | 1.850 | 1.750 | Frontal area |
| $c_N$ | 0.28 | 0.28 | 0.31 | Lift drag |
| $c_d$ | **0.33** | **0.32** | **0.30** | Aerodynamic drag |
| P (hp) | **100** | **120** | **90** | Horsepower |

The parameters in bold refer to the vehicle's manual

ADAS on vehicles. Therefore, the assessment of the vehicles' passing process was investigated solely through the interaction between vehicle dynamics and road geometry, where decision passing distance was incorporated. The process, assuming free flow conditions, involves the contribution of three vehicles; namely the passing vehicle, the passed vehicle and the opposing vehicle.

All three vehicles have different motion characteristics, where the following criteria—assumptions were applied:

- the speed of all three vehicles never exceeds the posted speed of the roadway
- the motion of the passed vehicle is under steady state conditions with a speed value below the posted speed of the roadway, where this speed difference is termed as ΔV
- the motion of the opposing vehicle is also under steady state conditions with a speed value equivalent to the roadway's posted speed
- the passing vehicle's motion during the passing process is under acceleration mode; however, it's initial speed value at the starting phase is set equivalent to the relevant speed of the passed vehicle and increasing continuously until the roadway's posted speed is reached from which point beyond steady state conditions apply
- energy deficits at the driven axle (94% approximately of the nominal value, as already mentioned) combined with vehicle aging as well as the ability of the driver to perform by utilizing the maximum permissible horsepower rates reduce the available net engine horsepower; however such reduction (more than 10% in total) was disregarded and the nominal horsepower supply of the vehicle was assumed be equivalent to the one utilized
- the headway ($dist_1$) between the passing (front bumper) and the of the passed (front bumper) vehicles at the starting phase of the passing process was assumed 15 m [9.5 m as referenced in [18] + 5.5 m approximately for the passed vehicle's length]
- the headway ($dist_2$) between the passing (front bumper) and the passed (front bumper) vehicles at the ending phase of the passing process was assumed 30 m [24 m as referenced in [18] + 6 m approximately the passing vehicle length]
- the safety margin was set to the constant value of 100 m [6], which actually can be interpreted as a safety margin of approximately 3.5 s for 100 km/h speed

The above mentioned distance criteria of the passing process are shown in Fig. 2.

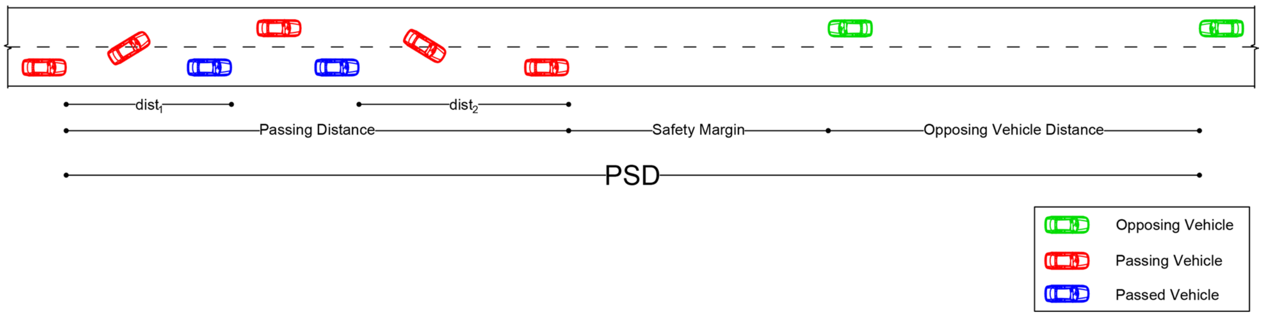


**Fig. 2** Distance criteria utilized for PSD determination


**Fig. 3** Coded targets mounted on the passed vehicle surface

### 3.3 Field measurements: validation

The field measurements were carried out on two mild graded (1.00% and 2.00%) 2-lane rural road sections located at Spata area (near Athens) for both directions of travel. The recording device used for the speed-distance data was the Vericom VC4000 accelerometer [32]. The peak friction supply for the examined road section was measured under dry road surface conditions $f_{MAX} = 0.82$. More information regarding both speed-distance and friction recording procedures through the accelometer, can be found in a similar research of the authors [22].

Due to the fact that the opposing vehicle's speed as well as the safety margin were considered constant for the same roadway, the validation of the process was concentrated in assessing the passing distance between the passing and the passed vehicles.

The key concept of the approach was the flexibility and the ease of the measuring process keeping it as cost effective as possible. Therefore, a HD machine-vision camera was utilized, mounted on the passing vehicle and recording continuously the passed vehicle during the maneuver. By that means, the distance among the two vehicles may be estimated for every successive frame, utilizing a typical image-based camera localization method that exploits tracked image features.

The overall robustness of this single camera approach was ensured by an accurate camera pre-calibration step, along with an a-priori 3D photogrammetric reconstruction of several signalized targets (coded targets) mounted on the passed vehicle surface as seen through Fig. 3. The achieved localization accuracy $\sigma$ is directly related to the distance (dist) from the camera towards the target-vehicle and ranges from some millimeters at close distances (dist < 5 m), to several centimeters at longer distances (e.g. $\sigma = \pm 10$ cm for dist > 10 m).

Figure 4 illustrates the process for the utilized time frame of 0.50 s ($\Delta t = 0.50$ s). The relative distance D traveled during the timeframe of $\Delta t$ (between $t_i$ and $t_i + \Delta t$) can be calculated from the distances between the passing and the passed vehicles, where having in mind their accelerating and steady state motion respectively, the following equations apply:

$$\begin{aligned} D &= dist_{t=t_i} + V_{o,passed}\Delta t \\ &= dist_{t=t_i+\Delta t} + V_{o,passing(t=t_i)}\Delta t + \frac{1}{2} a_i \Delta t^2 \end{aligned} \tag{3}$$

$$V_{o,passing(t=t_i+\Delta t)} = V_{o,passing(t=t_i)} + a_i \Delta t \tag{4}$$

where $a_i$: instant passing vehicle acceleration (m/s$^2$), $V_{o,passed}$: constant speed of the passed vehicle (m/s), $V_{o,passing}$: initial speed of the passing vehicle [$t = 0$: $V_{o,passing} = V_{o,passed}$] (m/s)

From Eq. 3 the instant acceleration $a_i$ can be defined. By substituting $a_i$ in Eq. 4, the speed $V_{o,passing(t=ti+\Delta t)}$ of the passing vehicle at the ending (beginning) of time frame $t_i$ ($t_i + \Delta t$) can be calculated. However, the achieved accuracies of distance measurements, (given estimation) though sufficient for close distances, yield inaccurate estimations of speed and acceleration at somewhat longer distances.

Nevertheless, the exploitation of Computer Vision techniques based on camera recordings remains a critical issue for speed estimation, in the sense that it can meet

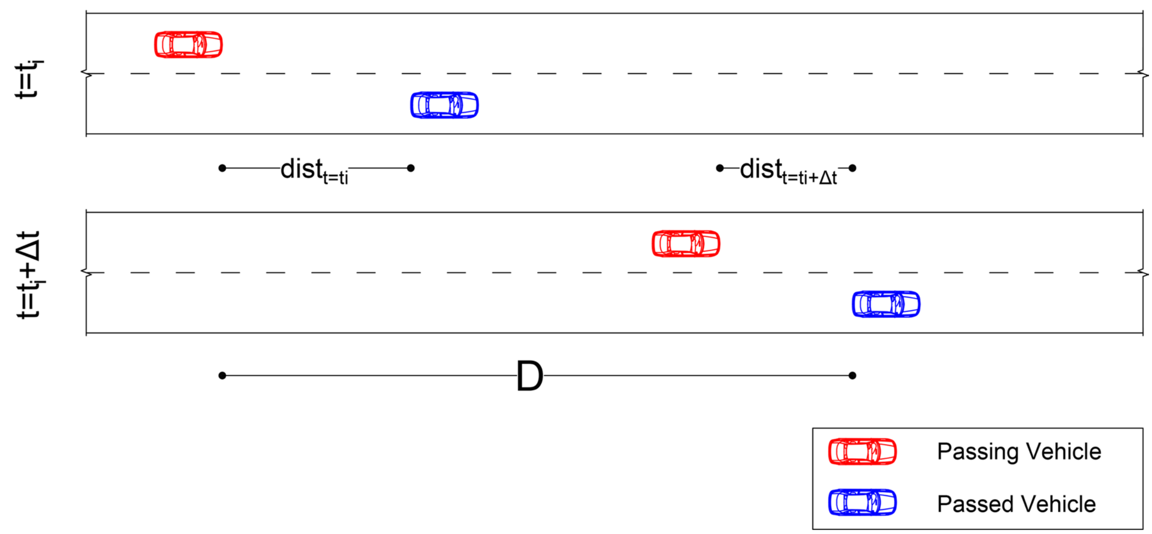


**Fig. 4** Relative positions of the passing and the passed vehicles for Δt = 0.5 s

and exceed the accuracy demands of this approach. This is feasible by leveraging different camera configuration scenarios and processing methods (e.g. synchronized recordings from multiple stationary and moving cameras, employment of a long-base stereo camera on board, integration of a visual system with data from various sensors such as Lidar, GPS/INS and Radar). In this context, it is worth mentioning that the case of simultaneous video recording from multiple cameras installed on the ground and on board of the vehicle, may yield an essential increase in the final accuracy of this approach. Hence, it could exceed significantly the corresponding results from single-device units such as single-camera monitoring systems or mobile mapping systems consisting of a single camera and Lidar sensor.

Therefore, the validation of the passing process was limited in correlating the passing vehicle's motion under acceleration between field data and the outputs of the vehicle dynamics model. Since the speed of the passed vehicle is considered constant, once the performance under acceleration of the passing vehicle is known, the relative distance between the passing and the passed vehicle can be easily figured out.

The validation was performed by correlating the acceleration performance of B Class (7 year old Toyota Yaris Diesel, manual gear) and C Class (brand new Toyota CH-R, automatic transmission) passenger cars against the vehicle dynamics model. The utilized parameters by vehicle can be seen through Table 2, where the initial speed values ($V_o$, at steady state conditions) were engaged from the accelometer in order to avoid vehicle odometer errors. However, in order to take into consideration more realistic situations (vehicle aging, energy deficits), the applied horsepower rates differed slightly as follows: 80hp for Toyota Yaris (90 hp × 90%) and 112hp for Toyota CH-R (120 hp × 94%).

The results are shown through Fig. 5a, b, where it can be seen that the automatic transmission vehicle delivers a better fit against vehicle dynamics model outputs (Fig. 5b). More specifically, in Fig. 5a the gearshift area, approximately 70 m from the starting point, generates a sort of delay in vehicle performance. However, in general the assessed speed distance correlation, especially for the automatic transmission vehicle, were found satisfactory, having in mind that optimum vehicle handling was assumed (human factor ignored).

In every case, a more advanced photogrammetric-based validation process is necessary in order to assess also potential impact from vehicle steering during the passing process, which within the present analysis was ignored.

## 4 Analysis

Aiming to utilize a uniform approach for assessing PSDs, the current analysis was performed in line with the design classes of German (RAL, 2012) rural road design guidelines, where, as already stated, PSD is currently dependent on the homogeneity of the proposed road design classes and no longer on speed. In RAL 2012 guidelines, four design classes are introduced; namely, EKL1, EKL2, EKL3 and EKL4 with varying design speeds, cross sections and control design elements. However, EKL1 design class, with design speed V = 110 km/h, was excluded from the present analysis, since the passing process is performed only through additional passing lanes. EKL 4 design class (with 70 km/h design speed) was also

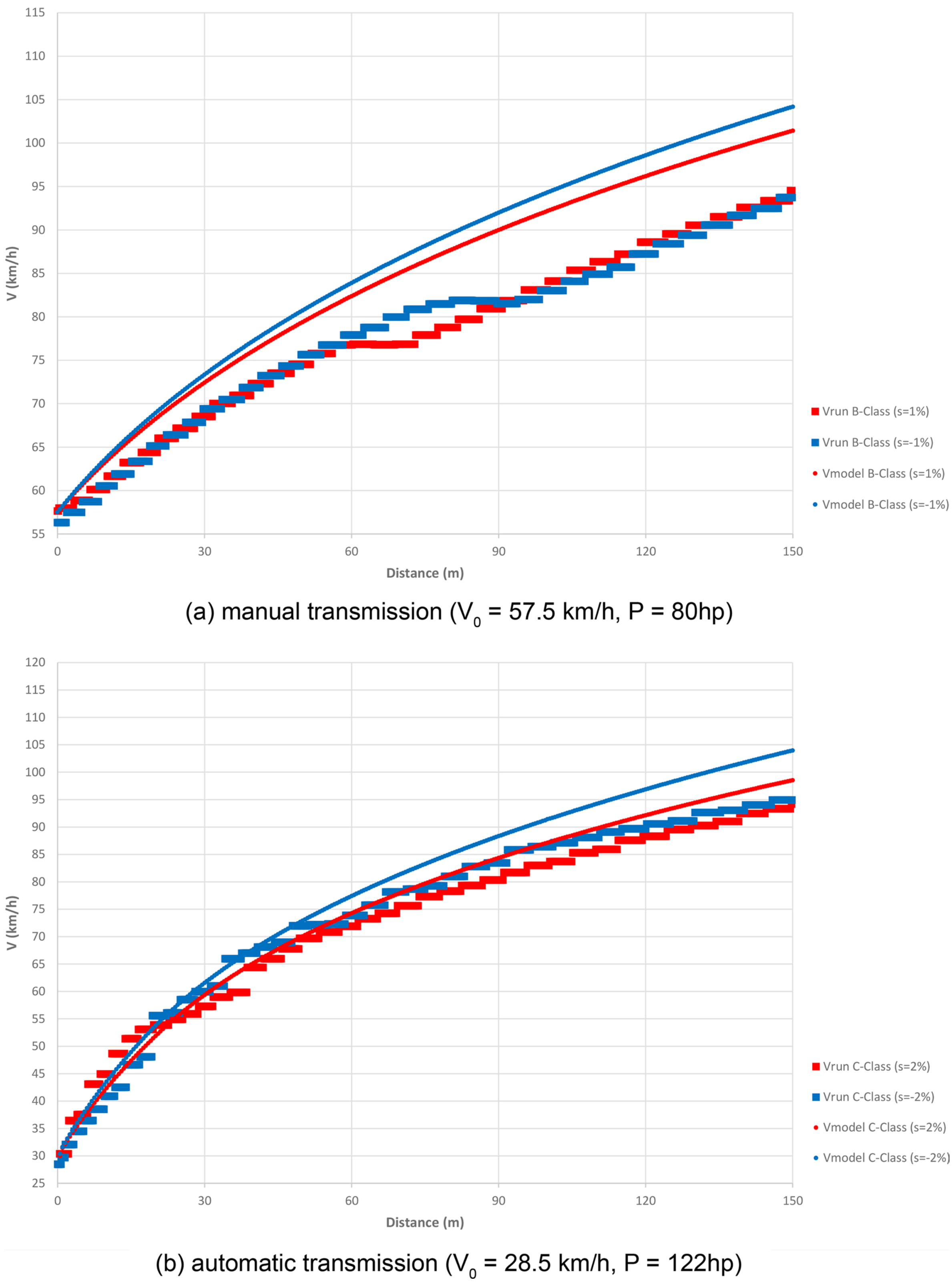


**Fig. 5** **a**, **b** Acceleration performance correlation between field data—vehicle dynamics model

**Table 3** Control values for RAL, 2012 (18)

| Design class | Design speed V (km/h) | Grade s (%) | PSD (m) |
|---|---|---|---|
| EKL2 | 100 | 5.50 | 600 |
| EKL3 | 90 | 6.50 | 600 |

excluded since the respective cross section that applies refers to a single 6.00 m carriageway serving both directions of travel. The examined design classes as well as the utilized control values of speed, grade and PSD requirements are shown in Table 3.

The proposed PSD assessment was implemented for EKL2 and EKL3 design classes (2 lane rural roads) with posted speed values of 100 km/h and 90 km/h respectively. Moreover, the following parameters from the vehicle—roadway interaction were used:

The vehicle nominal (also assumed as utilized) horsepower rate, where three different rates were utilized: 80 hp, 100 hp and 120 hp.

Pavement friction, where three values of peak friction supply coefficients $f_{max}$ were used (0.35, 0.50 and 0.65). Since the sliding friction coefficient and consequently the relevant peak value are subject to excessive variations in terms of wet-dry pavement conditions, the intention was to assess pavements with poor friction performance under both wet (0.35) and dry (0.65) pavement conditions.

The potential grade impact during vehicle passing performance was also investigated. For each design class, in accordance with Table 3, three different grade values were investigated (max. upgrade, level and max. downgrade).

Finally, per examined design class, as the speed of the opposing vehicle was always set to the value shown in Table 3, three different speed values for the passed vehicle were investigated; namely, 10 km/h, 20 km/h and 30 km/h below the respective design speed value.

Summarizing, certain cases by design class were examined by arranging the combinations of the above mentioned 4 independent variables; namely, vehicle horsepower rates [P (hp)], difference between passed vehicle's speed (also initial speed of passing vehicle) and roadway's posted—design speed [ΔV (km/h)], peak friction supply coefficients ($f_{max}$), and grade values [s (%)]. Every independent variable came along with 3 different values, where in total, 81 different cases per design class were examined.

The developed PSD graphs delivered various interesting findings although some of them can be reached rather straightforward.

As expected, the dominant parameter that mostly affected PSD was found to be the speed differential parameter ΔV, where for all the examined cases, the analysis revealed that the passing vehicle was able to reach the posted speed of the roadway.

When a vehicle with low horsepower rate is driven at impending skid conditions ($n < 100\%$), the passing performance for a vehicle with the same initial road—vehicle parameters but with greater horsepower rate remains the same.

In cases where a vehicle for a certain pavement friction outperforms (reaches 100% of its nominal horsepower rate, $n = 100\%$) at the beginning of the passing process, even when the vehicle performs on improved pavement, in terms of friction, the vehicle will still necessitate the same PSD. An exception is noticed when the vehicle outperforms during the passing process.

Figure 6a, b illustrate two distinctive cases; the interaction of the remaining independent variables on PSD by retaining the roadway's grade and friction values respectively. Moreover, in both figures the sum of the passing maneuver under both acceleration and posted speed status deliver the passing zone per examined case.

In Fig. 6a, it can be seen that between the two extreme horsepower rates assessed, PSD has a moderate difference of approximately 20 m on the most favorable in terms of friction pavement ($f_{max} = 0.65$) which vanishes as $f_{max}$ decreases.

On the other hand, as seen through Fig. 6b, the grade impact, between the two extreme grade values assessed, is more noticeable on the vehicle with the lowest horsepower rate (approximately 20 m for P = 120hp vs 35 m for P = 80 hp).

Among the most important findings is the excess of the 600 m PSD requirement. This is mostly evident for cases where the speed of the passed vehicle is below 20 km/h from the roadway's posted speed. Especially for EKL2 design class (Fig. 6a), when ΔV was set to 20 km/h, it was found that the demanded PSD slightly exceeded 600 m (s = 0%).

Another interesting outcome is the fact that solely the examined horsepower supply of the vehicles has a rather moderate impact on the final PSD. This is explained as follows; the vehicle supplied with the higher horsepower rate reaches the posted speed travelling a shorter distance. Comparing the two extreme cases of 80 hp and 120 hp, the vehicle equipped with 80 hp travels approximately 40% more distance (blue bars in Fig. 6b) in order to reach the roadway's posted speed. This means that when both vehicles reach the posted speed value, the 80 hp vehicle, compared to the passed vehicle has shorter relative distance to complete the passing maneuver than the 120 hp vehicle (varies approximately 10–30 m,

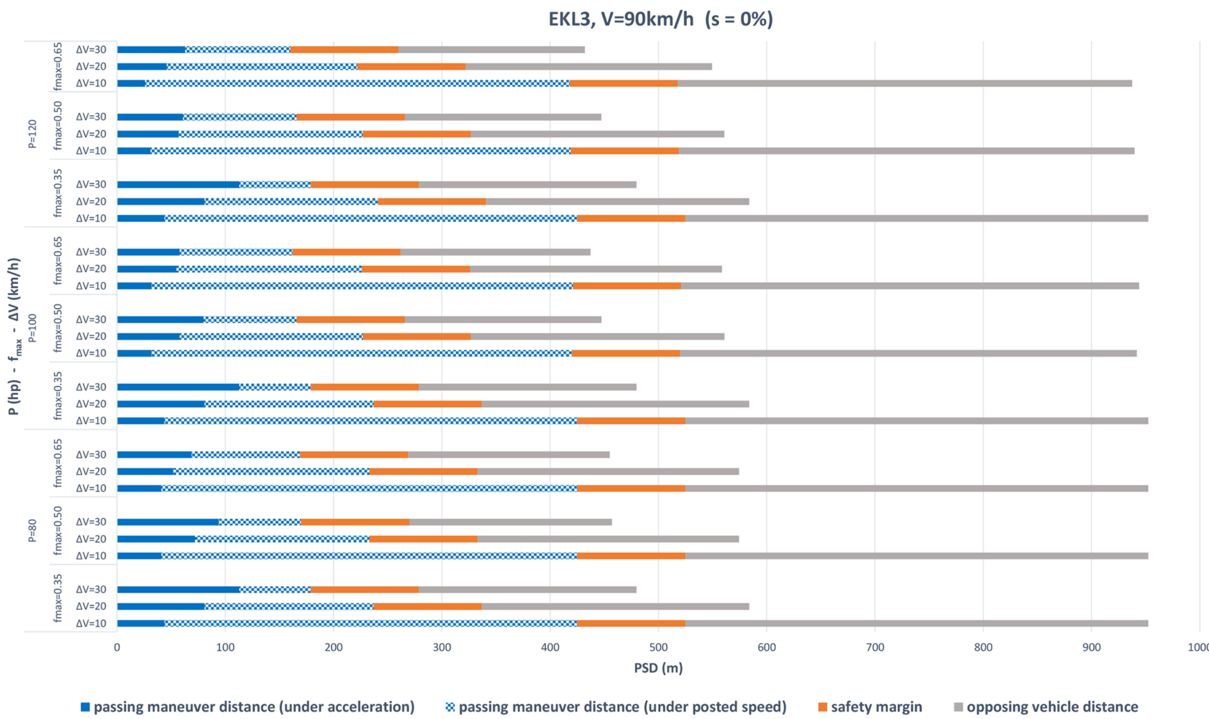


(a) EKL2, V = 100 km/h, s = 0%

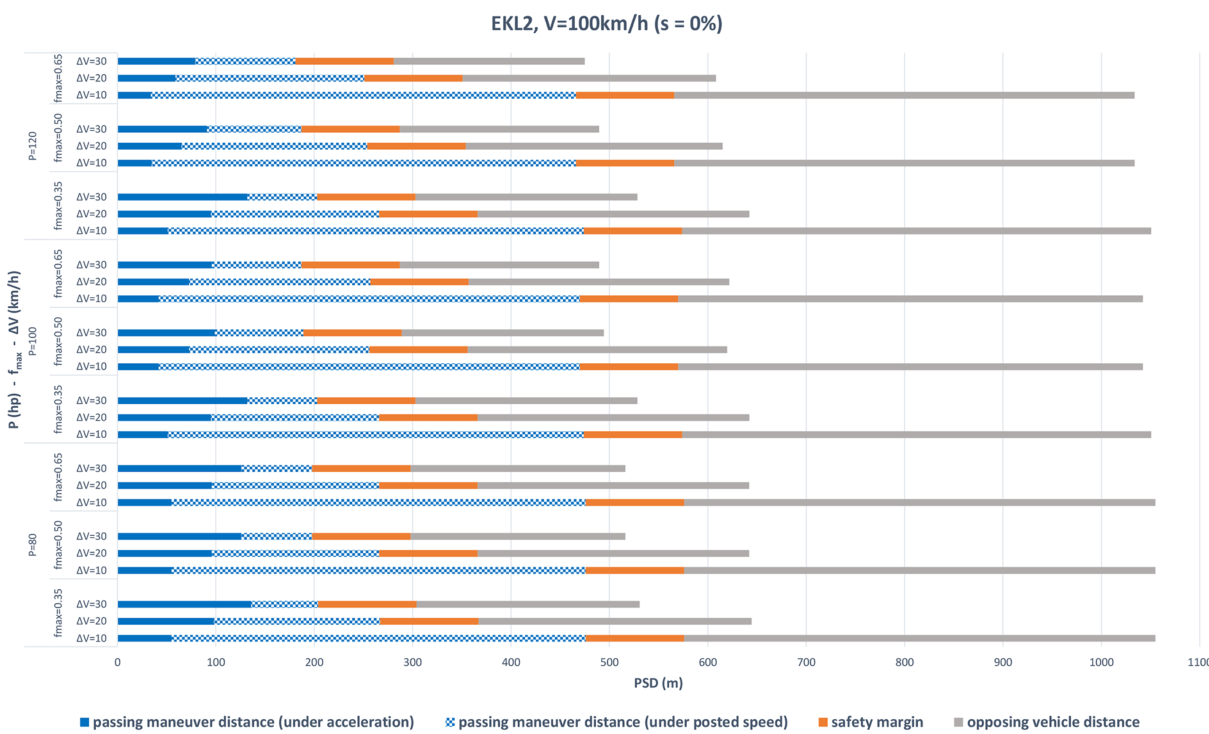


(b) EKL3, V = 90 km/h, $f_{max}$ = 0.65

**Fig. 6** **a**, **b** Interaction of road—vehicle parameters during PSD determination depending on grade and ΔV). As a result, the passing maneuver distance per vehicle with 80 hp and 120 hp is somehow balanced.

### 4.1 Lognormal regression modelling of PSD

The specification of the required PSD model was determined on the basis of a thorough descriptive analysis of the data revealing nonlinear associations of PSD with the examined variables. A histogram of the response variable led to the identification of a clearly skewed density function, suggesting a lognormal distribution (Eq. 5). Consequently, with $X_i$ the explanatory variables, $\beta_i$ parameters to be estimated and $\varepsilon_i$ the normally distributed ~ $[0, \sigma^2]$ error term, this lognormal model is formed as follows:

$$\log(PSD_i) = \sum \beta_i \cdot X_\iota + \varepsilon_i \tag{5}$$

The parameter estimates and goodness-of-fit measures of the best fitting model are presented in Table 4. The final model is specified for each examined road class (EKL2, EKL3) separately:

EKL2 Design Class:

$$\log(PSD) = 3.1915 - 0.01555\Delta V - 0.0007P\ f_{max} + 0.00018s\ \Delta V \tag{6}$$

**Table 4** (a, b) Parameter estimates and goodness-of-fit of the lognormal regression model of PSD

| Parameter | B | Std. Error | t-value | *p* value |
|---|---|---|---|---|
| *(a) EKL2* | | | | |
| (Intercept) | 3.19150 | 0.01520 | 209.949 | < 0.001 |
| ΔV | − 0.01555 | 0.00043 | − 35.750 | < 0.001 |
| P $f_{max}$ | − 0.00070 | 0.00024 | − 2.949 | 0.004 |
| s ΔV | 0.00018 | 0.00004 | 4.808 | < 0.001 |
| Null log-likelihood | | 48.947 | | |
| Final log-likelihood | | 166.033 | | |
| Likelihood ratio test | | 2.443 | | |
| df | | 3 | | |
| Adjusted R-squared | | 0.942 | | |
| *(b) EKL3* | | | | |
| (Intercept) | 3.15000 | 0.01532 | 205.567 | < 0.001 |
| ΔV | − 0.01560 | 0.00044 | − 35.588 | < 0.001 |
| P $f_{max}$ | − 0.00072 | 0.00024 | − 3.006 | 0.00357 |
| s ΔV | 0.00015 | 0.00003 | 4.775 | < 0.001 |
| Null log-likelihood | | 48.641 | | |
| Final log-likelihood | | 165.389 | | |
| Likelihood ratio test | | 2.448 | | |
| df | | 3 | | |
| Adjusted R-squared | | 0.944 | | |

EKL3 Design Class:

$$\log(PSD) = 3.1500 - 0.01560\Delta V - 0.00072P\ f_{max} + 0.00015\ s\Delta V \tag{7}$$

In this case, this model can be analyzed, based on variables and interactions for all the examined alignments (e.g. ΔV, $P \times f_{max}$, s × ΔV). Furthermore, a quadratic function of gradient (s) and horsepower (P) was tested but was not found to outperform the logarithmic function with respect to PSD. A collinearity test was conducted, to ensure that the independent variables were not correlated with each other.

The parameter estimates of the main effects suggest that an increase in one interaction (e.g. s × ΔV) increase passing sight distance, while on others (e.g. ΔV, $P \times f_{max}$) decrease PSD. The likelihood ratio test leads to accept the model compared to the null model, and an adjusted R-squared is equal to 0.94 in both cases, which is satisfactory.

A closer look at the predicted values suggest that the differences between observed and predicted values are low; however, the model residuals are not white noise (e.g. unrelated to the predicted values), and the plot of residuals against the predicted values suggests the presence of a more complex non-linear relationship.

It is clear that the final model specification may not address all possible combinations of design parameters with the same accuracy and the lognormal model is certainly an approximation. However, even with this imperfect specification, the model can be useful within a preliminary assessment of the design parameters as regards PSD.

## 5 Discussion and conclusions

The present paper investigated the interaction between vehicle dynamic parameters and road geometry during the passing process. Regarding road geometry it should be stressed that in current design practice passing distance data were delivered with respect to the roadway's posted speed as well as the ability of the examined (passing) vehicle to perform such maneuvers.

At present time, the compliance with the posted speed during vehicle passing is not realistic. However, the assessment refers to how the passing process can be standardized and therefore deployed in existing ADAS. This effort is at preliminary stage since the speeds of the passed and the opposing vehicles were considered constant but also traffic conditions were assumed ideal (free flow).

An imminent challenge is to further improve the described methodology by enabling more sophisticated communication between vehicles (V2V) or between vehicles and road environment (V2I) and thus enable the utilization of guidance during the passing process in an advanced vehicle automation levels environment. During such an effort, cases of unforeseen situations that might cancel the passing process should be also addressed. Such cases, among others, include the capability of obstacles detection on the roadway through cameras with deep learning process, tire—road friction assessment due to harsh weather conditions, etc.

The analytical model, although delivers accurate passing distance outputs, especially for automatic transmission vehicles, is computationally demanding and therefore a statistical modelling approach was worked out by utilizing 4 vehicle—roadway variables with very satisfactory precision. The derived models may be useful to researchers and practitioners aiming to determine PSDs as well as passing zones by assessing the interaction of road—vehicle parameters. In this view, the PSD models can be also used as a basis for supporting the design of markings and signs. More specifically, by selecting reference $\Delta V$ and vehicle engine horsepower (P) values, the adequacy of existing or under design passing zones can be assessed more evidently, especially for areas with steep grades and/or poor pavement friction. Moreover, regarding the latter, the need for utilizing variable message signs can be justified more accurately.

Although the impact of (standing alone) vehicle horsepower rates (at least the examined values) on the passing process was rather moderate, the speed difference ($\Delta V$) between the passed vehicle and the posted speed value was found to impact excessively PSD, especially for $\Delta V < 20$ km/h. In every case, further research is necessary to quantify more accurately the amount of utilized horsepower rates during passing maneuvers.

A related issue of great importance to be further investigated, mainly for $\Delta V = 10$ km/h, is the potential impact on the roadway's operational level, since unless the vehicle to be passed further decreases it's speed, the roadway is subject to perform below the designed level of service. Therefore, in partial automation environment (e.g. Level 2), the required PSDs are not expected to reduce. In more advanced V2V automation environment, such a reduction seems feasible; however, the vehicles interaction necessitates deeper investigation.

In addition, since only a partial range of passenger cars was examined, further work is required to incorporate representative vehicles from the vehicle fleet (SUVs, sport vehicles, heavy vehicles, etc.) in order to examine more thoroughly passing assessments as well as critical barriers that may emerge (e.g. sight distance limitations during truck passing). Moreover, the impact of road geometry in terms of curvature (both horizontal and vertical) as well as intersections areas are also challenging fields.

Concluding, it should not be ignored that the human factor during the acceleration process might impose additional restrictions and, consequently, affect vehicle's safety performance.

**Acknowledgements**
Not applicable.

**Author contributions**
The authors confirm contribution to the paper as follows: study conception and design: SM and VM; data collection: SM, VM, and KA; analysis and interpretation of results: SM, VM and KA; draft manuscript preparation: SM, VM, KA, FF and GY. All authors reviewed the results and approved the final version of the manuscript.

**Funding**
Not applicable.

**Availability of data and materials**
The datasets used and analyzed during the current study are available from the corresponding author on reasonable request.

## Declaration

**Competing interests**
Not applicable.

Received: 1 August 2022 Accepted: 8 March 2023
Published online: 15 March 2023

**References**

1. American Association of State Highway and Transportation Officials (AASHTO). (2018). *A policy on geometric design of highways and streets*, 5th edition. Washington, DC.
2. Belz, N. (2019). Using field and simulation data to assess passing zone behavior on rural two lane highways. In *98th annual meeting of the transportation research board*, Washington, DC.
3. Carlson, P., Miles, J., & Johnson, P. (2006). Daytime high-speed passing maneuvers observed on rural two-lane, two-way highway: Findings and implications. *Transportation Research Record, 1961*, 9–15.
4. Clarke, D. D., Ward, P. J., & Jones, J. (1998). Overtaking road-accidents: differences in maneuver as a function of driver age. *Accident Analysis & Prevention, 30*(4), 455–467.
5. Dixon, J. C. (1996). *Tires, suspension and handling* (2nd ed.). Warrendale, PA: Society of Autimotive Engineers, Inc.
6. Ed.German Road and Transportation Research Association, Committee. (2012). *Geometric design standards. Guidelines for the design of rural roads, (RAL)*, Germany.
7. Edwards, C. H., Jr., & Penney, D. E. (1996). *Differential equations and boundary value problems: Computing and modeling*. Prentice-Hall.
8. Farah, H. (2011). Age and gender differences in overtaking on two-lane rural highways. In *90th annual meeting of the transportation research board*, Washington, DC.
9. Federal Highway Administration FHWA. (2014). Safety effects of horizontal curve and grade combinations on rural two-lane highways (FHWA-HRT-13-077). Office of Safety Research and Development, VA.
10. Forbes, G. J. (1990). Origin of minimum passing sight distances for no-passing zones. *ITE Journal (Institute of Transportation Engineers), 60*(12), 20–24.
11. Garcia, A., Llopis Castello, D., & Camacho Torregrosa, F. J. (2019). Influence of the design of crest vertical curves on automated driving experience. In *98th annual meeting of the transportation research board*, Washington DC.

12. Gillespie, T. D. (1992). Fundamentals of vehicle dynamics. *Society of Mining Metallurgy and Exploration*.
13. Harwood, D., Gilmore, D., & Richard, K. (2010). Passing sight distance criteria for roadway design and marking. *Transportation Research Record: Journal of the Transportation Research Board, 2195*, 36–46.
14. Harwood, D. W., & Mason, J. M. (1994) Horizontal curve design for passenger cars and trucks. *Transportation Research Record 1445*, Transportation Research Board, Washington DC (pp. 22–33).
15. Heisler, H. (1993). *Advanced vehicle technology*. Edward Arnold. A Division of Hobber & Stoughton.
16. Llorca, C., & Farah, H. (2016). Passing behavior on two-lane roads in real and simulated environments. *Transportation Research Record: Journal of the Transportation Research Board, 2556*(1), 29–38.
17. Llorca, C., & García, A. (2011). Evaluation of passing process on two-lane rural highways in Spain with new methodology based on video data. *Transportation Research Record: Journal of the Transportation Research Board, 2262*(1), 42–51.
18. Llorca, C., Moreno, A., García, A., Pérez-Zuriaga, A. M., & Camacho Torregrosa, F. J. (2013) Multiple passing maneuvers: New design and marking criteria to improve safety. *Road Safety and Simulation International Conference, RSS2013.* Rome, Italy.
19. Mavromatis, S., & Psarianos, B. (2003). Analytical model to determine the influence of horizontal alignment of two-axle heavy vehicles on upgrades. *Journal of Transportation Engineering, 129*(6), 583–589.
20. Mavromatis, S., & Markos, K. (2022). Passing sight distance assessment on rural roads with crest vertical curves. In *Proceedings of the 6th international symposium on highway geometric design TRB*, Amsterdam, Netherlands.
21. Mavromatis, S., Laiou, A., & Yannis, G. (2019). Safety assessment of control design parameters through vehicle dynamics model. *Accident Analysis and Prevention, 125*, 344–351.
22. Mavromatis, S., Laiou, A., Yannis, G., & Psarianos, B. (2018). Acceleration impact investigation for control road geometry parameters. In *97th annual meeting of the transportation research board*, Washington, DC.
23. Mavromatis, S., Papadimitriou, E., Yannis, G., & Psarianos, B. (2017). Vehicle skidding assessment through maximum attainable constant speed investigation. *Journal of Transportation Engineering, American Society of Civil Engineers Part A: Systems, 143*(9), 04017044.
24. Mavromatis, S., Psarianos, B., D'Apuzzo, M., & Nicolosi, V. (2000). Design speed ranges to accommodate a safe highway geometric design for heavy vehicles. In *Transportation research board. 2nd international symposium on highway geometric design*, Mainz, Germany (pp. 339–351).
25. Molinero, A., Carter, E., Naing, C., Simon, M., & Hermintte, T. (2008). Accident causation and pre-accidental driving situations. Part 1. Overview and general statistics. *TRACE—Traffic accident causation in Europe report*.
26. Pérez-Zuriaga, A. M., Camacho Torregrosa, F. J., García, A., Llorca, C., & Moreno, A. (2013). Analyzing speeding behavior in two-lane rural roads. In *Road safety and simulation international conference, RSS2013.*Rome, Italy.
27. Persaud, B. N., Retting, R. A., & Lyon, C. A. (2004). Crash reduction following installation of centerline rumble strips on rural two-lane roads. *Accident Analysis & Prevention, 36*, 1073–1079.
28. Polus, A., Livneh, M., & Frischer, B. (2000). Evaluation of the passing process on two-lane rural highways. *Transportation Research Record: Journal of the Transportation Research Board, 1701*, 53–60.
29. Richter, T., & Ruhl, S. (2014) Untersuchung von Maßnahmen zur Prävention von Überholunfällen auf einbahnigen Landstraßen, [Examination of Measures to Prevent Passing-Related Accidents on Two Lane Highways] *Gesamtverband der Deutschen Versicherer, Forschungsbericht*, No.24 [German Insurance Association, German Insurance Accident Research], Berlin.
30. Society of Automotive Engineers International. Taxonomy and Definitions for Terms Related to Driving Automation Systems for On-Road Motor Vehicles. (2016). *SAE international's on-road automated driving (ORAD) committee, United States*. Retrieved June 30, 2019, from https://saemobilus.sae.org/content/J3016_201609.
31. Transportation Research Board (TRB). (2008). Passing sight distance criteria. *National Cooperative Highway Research Program (NCHRP)*, NCHRP Report 605, Washington, DC.
32. Vericom Computers (2010) Vericom VC4000DAQ. Performance and braking test computer, Rev.1.10. Vericom Computers Inc., Rogers, MN USA.
33. Vetters, A., & Jaehrig, T. (2015). Verification of the existing model for passing sight distance on single two-lane rural carriageways. In *6th IEEE international conference on cognitive infocommunications*. Győr, Hungary.
34. Younsi, K., Floris, J., Rajaonah, B., Simon, P., Loslever, P., & Popieul, J. C. (2011). Study of driver's behavior during overtaking situations. *Advances in Transportation Studies: An International Journal, 25*(A 25), 29–38.


## Publisher's Note